Application of the Plane-Faced-Energy-Surface Method to the Calculation of the Hall Effect in Hexagonal Alloy Phases

P. H. Cowley and J. Stringer
Department of Metallurgy and Materials Science, University of Liverpool, England
(Received 9 January 1973)

The plane-faced-energy-surface (PFES) method introduced by Allgaier has been used to calculate the two components of the low-field Hall tensor for hexagonal closed-packed ϵ and ζ phases having electron-to-atom ratios in the range 1.3–1.8. Two simple polygonal PFES have been chosen to represent the low electron-to-atom-ratio ($\vartheta < 1.45$) and high electron-to-atom-ration ($\vartheta > 1.6$) regions, and the results of the calculations, which involve no arbitrary parameters apart from the choice of surface, are in very satisfactory agreement with the experimental results. An estimate of the effect of overlap at higher electron-to-atom ratios is made, and it appears that there is little or no overlap in the case of the ζ alloys, but there is clearly considerable overlap in the ϵ phases.

INTRODUCTION

In discussing the Hall effect in anisotropic media it is necessary to adopt a definition which clearly distinguishes it from the change in resistance due to a magnetic field. Following Logan and Marcus[1] we choose to adopt the convention that the Ohmic field is

$$\tfrac{1}{2}[\vec{E}(\vec{B}) + \vec{E}(-\vec{B})] \tag{1}$$

and the Hall field is

$$\tfrac{1}{2}[\vec{E}(\vec{B}) - \vec{E}(-\vec{B})] \tag{2}$$

so that the Hall field reverses its direction on reversing the direction of the applied magnetic field, while the Ohmic field does not. Further, the Hall field vanishes when $\vec{B} = O$. This choice is based on a calculation of Casimir,[2] who showed that, for an anisotropic material, if the vectors are resolved in any convenient rectangular coordinate system

$$E_i = \sum_j \rho_{ij} J_j + (\vec{r} \times \vec{J})_i \ , \tag{3}$$

where the ρ_{ij} are functions of $\vec{B}$ such that

$$\rho_{ij}(\vec{B}) = \rho_{ij}(-\vec{B})$$

while

$$\vec{r}(\vec{B}) = -\vec{r}(-\vec{B}) \ .$$

The vector $\vec{r}$ is called the Hall vector.

Kohler[3] analyzed the limitations imposed by crystal symmetry on the Hall vector. Writing

$$r_i = \sum_j R_{ij} B_j \ ,$$

the coordinate system is chosen so that one axis is parallel to the hexad axis of symmetry in the hexagonal system, and the other two are parallel to mutually perpendicular directions in the basal plane. In this case the matrix $\underline{R}$ is diagonal, and symmetry considerations together with the Onsager relationships indicate that only two of the diagonal terms are independent. These are labeled $R_\parallel$ and $R_\perp$, adopting the convention that $R_\parallel$ is the Hall coefficient when the magnetic induction is parallel to the hexad axis.

METHODS OF CALCULATION OF HALL EFFECT

In the simple free-electron model, it is easy to show that the Hall effect is isotropic, and

$$R = 1/ne \ , \tag{4}$$

where n is the number of carriers charge e per unit volume. In a more general weak-field (classical) model the calculation is much more difficult. Following Chambers[4] the conductivity tensor σ_{ij} may be written as

$$\sigma_{ij} = -\frac{e^2}{4\pi^3} \int v_i L_{E,j} \frac{\partial f^0}{\partial \epsilon} d\vec{k} \approx \frac{e^2}{4\pi^3 \hbar} \int v_i L_{E,j} dS_F / v \ . \tag{5}$$

The $L_{E,j}$ are the components of a vector $\vec{L}_{E,\vec{k}}$ which is the average distance travelled by an electron before passing through a given point in the metal with velocity $\vec{v}_{\vec{k}}$, and thus contains the scattering time (which is in general not a scalar). In the second form of Eq. (5) an approximation has been used to transform the integral over all $\vec{k}$ to an integral over the Fermi surface S_F.

In general, the integration in Eq. (5) must be performed numerically on the basis of accurate experimental information on the Fermi-surface topography, the velocity distribution over the Fermi surface, and the scattering time distribution over the Fermi surface. For the particular case of copper, where the topography and the velocities are well documented, Dugdale and Firth[5] have carried out the calculation using an isotropic scattering time and have obtained excellent agreement with experiment. However, for hexagonal metals the calculation is appreciably more difficult, and the

available experimental Fermi-surface data is much less detailed; for concentrated alloys the lack of any direct information makes the use of Eq. (5) out of the question.

However, recently Hitchock and Stringer[6] have shown that the Hall coefficients in a disordered hexagonal close-packed Cu-Ge alloy are qualitatively consistent with the mean curvatures of a "reasonable" Fermi surface. This is an extremely simple case, since the Fermi surface is probably still confined to the first zone, and the dominance of impurity scattering means that the assumption of an isotropic relaxation time is reasonable. For this reason, it is clearly worth exploring the possibility of carrying out a more exact quantitative calculation.

Tsuji and Kunimune[7] have carried out a detailed calculation of the transport properties of cadmium using a model Fermi surface approximating the complex experimental surface, but neglecting relaxation anisotropy. The agreement with experiment was poor, although the calculation was capable of producing anisotropies of the right order.

In fact, it is clear that attempts to calculate the Hall effect in terms of Eq. (5) or any similar approximation for disordered hexagonal alloys will (a) be extremely difficult; (b) contain a large number of disposable parameters, in the sense that direct experimental information is not obtainable; and (c) lack the flexibility necessary for interpretation of data produced from a wide range of alloy systems.

In this paper, we explore the possibility of using the plane-faced-energy-surface (PFES) method introduced by Allgaier.[8-10] This novel approach does not appear to have been applied to the interpretation of the Hall coefficient in alloys, but it has the virtue of simplicity in the number and type of calculations required, and aspects such as varying velocity and relaxation time can be easily introduced.

The PFES Method

In principle, the method replaces the real Fermi surface by a polyhedron bounded by plane faces. So long as a carrier remains on one face, it makes no contribution to the Hall effect, but as it drifts across the edge of a face it effectively rotates its momentum vector through a relatively large angle, thus contributing to the rotation of the overall current vector and producing a Hall effect. The calculation thus consists of determining the shift in the polyhedron due to the application of the external forces, and hence the number of carriers which must move across an edge to produce the necessary shift.

The method of calculation can be shown as follows (the illustration is taken directly from Allgaier[9] and is in terms of the motion of *positive* charges).

Figure 1 shows a cubic Fermi surface of edge length $2p$ in momentum space, centered on the origin. The electric field is applied along the x axis, and produces the displacement Δp_x indicated by the dashed lines:

$$\Delta p_x = eE_x\tau \ . \tag{6}$$

The longitudinal current produced by the displaced carriers is the product of (a) the carrier density in the newly occupied and newly vacated states, (b) the charge e, and (c) the velocity v_x on the top face of the Fermi surface:

$$i_x = (2/h^3)(8p^2eE_x\tau)(ev_x) \ . \tag{7}$$

Now, if a magnetic field H_z is applied along the z axis, the Lorentz force causes a portion of the displaced distribution, indicated by the dotted lines in Fig. 1, to drift across the upper right edge of the Fermi surface, and thus produce a transverse current, and there is an equal contribution from the lower left edge. The transverse displacement is

$$\Delta p_y = ev_xH_z\tau \tag{8}$$

and the transverse current is then

$$i_y = (2/h^3)(4peE_x\tau)(ev_xH_z\tau)(ev_y) \ . \tag{9}$$

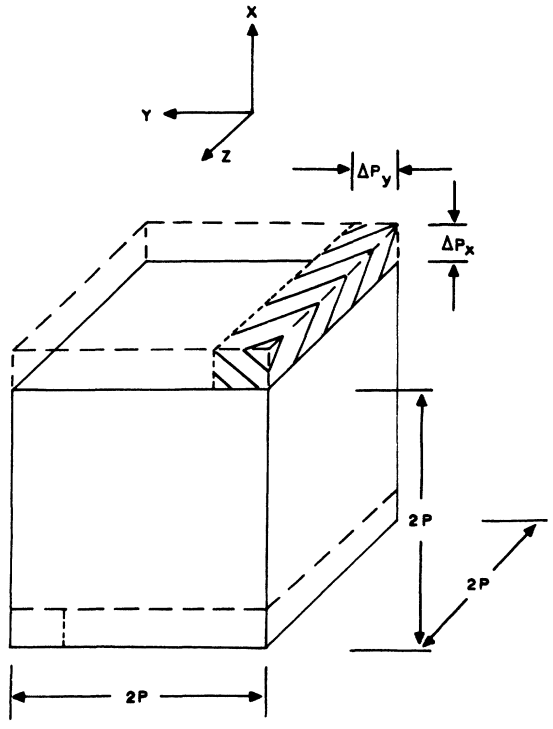

FIG. 1. Displacements produced by applied fields on a cubic PFES.

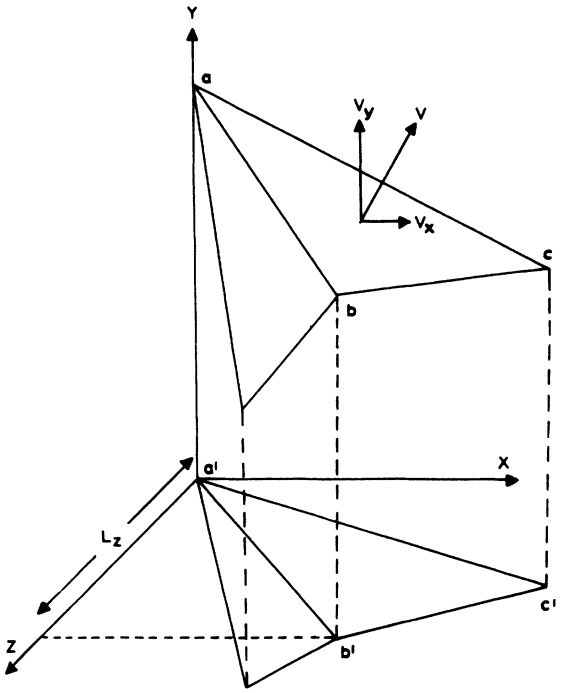

FIG. 2. A pair of oblique faces meeting in an oblique edge *ab* and their projection on the *xz* plane.

The Hall coefficient R_0 is then

$$R_0 = \frac{E_H}{i_x H_z} = \frac{E_x(-i_y)}{i_x^2 H_z} = -\frac{h^3}{32p^3 e}\frac{v_y}{v_x} , \tag{10}$$

and writing

$$n = (2/h^3)(2p)^3 ,$$

we get

$$R_0 = \frac{1}{2ne}\frac{v_y}{v_x} , \tag{11}$$

which, in the special case of $v_x = v_y$ is exactly half the value for a spherical surface. This result has been obtained for a cubic surface using the more traditional kinetic method by Goldberg *et al.*[11]

The procedure for calculation based on a more general polyhedral surface can be illustrated by considering two adjacent, oblique faces, intersecting in an oblique edge, as shown in Fig. 2. The contribution to i_x from a given face is determined from the x component of the velocity on the face, and the volume swept out as it is displaced in the p_x direction. This volume is $eE_x\tau$ times the *projected* area A^1 of the face on the p_y-p_x plane.

Thus, for face 1 and the face related to it by inversion,

$$i_x(1) = (2/h^3)(2eE_x\tau A^1)(ev_{1,x}) . \tag{12}$$

Similarly, the contribution to i_y from the volume of carriers crossing a particular edge is computed from three projected lengths: the projection of the edge length on the p_y-p_z plane, the p_x displacement $eE_x\tau$ and the p_y component of the displacement along the face due to the Lorentz force. The displacement generally involves both v_x and v_y components of the velocity on the face $\vec{v}$, but only v_x appears in the p_y projection. Also required is the *change* in v_y going from the initial to the final face.

Thus in Fig. 2, the contribution to i_y from the carriers passing from face 1 to face 2 across the edge $p_a p_b$, and from the two faces related to them by inversion is

$$i_y(1-2) = (2/h^3)(p_{bz} - p_{az})(2eE_x\tau)(ev_{1,x}H_z\tau) \times (e)(v_{2,y} - v_{1,y}) . \tag{13}$$

In these expressions, the relaxation time τ has been assumed to be isotropic. However, anisotropic scattering can be introduced into the model quite simply. If τ is assumed constant along the edges, but changes towards the center of a face, the effect is to increase or decrease the influence of the edges. For a general surface one could in addition introduce constant, but different, values of τ for the various nonequivalent types of face.

Finally, therefore, the various contributions to i_x and i_y from the different faces of the polyhedron are calculated using Eqs. (12) and (13) and summed. Commonly, the symmetry of the polyhedron reduces the number of calculations that have to be performed to less than ten, even for quite involved polyhedra. The Hall coefficient is then calculated from Eq. (10), and for an anisotropic material it is only necessary to rotate the polyhedron with respect to the experimental coordinate system and repeat the calculations to determine the various components. The form of Eq. (10) is slightly altered, however, and becomes[10]

$$R_0 = E_x(-i_{yx})/i_x i_y H_z , \tag{14}$$

where now the currents i_x and i_y are those which result when the electric field $\vec{E}$ is applied in the positive x and y directions, respectively, with $H_z = 0$. The Hall current i_{yx} results when $\vec{E}$ is in the x direction and $H_z \neq 0$. The Hall current i_{yx}, it must be remembered, is *entirely* due to carriers which drift across an edge, and is just the current i_y in the isotropic case [Eq. (13)].

For hexagonal crystals, $R_0 = R_\parallel$ when the hexad axis is parallel to the z axis, and thus the x and y directions both lie in the basal plane: clearly in this case $i_x = i_y$. However, $R_0 = R_\perp$ when the z axis lies in the basal plane, and in this case either the x or y axis is parallel to the hexad axis and the other also lies in the basal plane. For this situa-

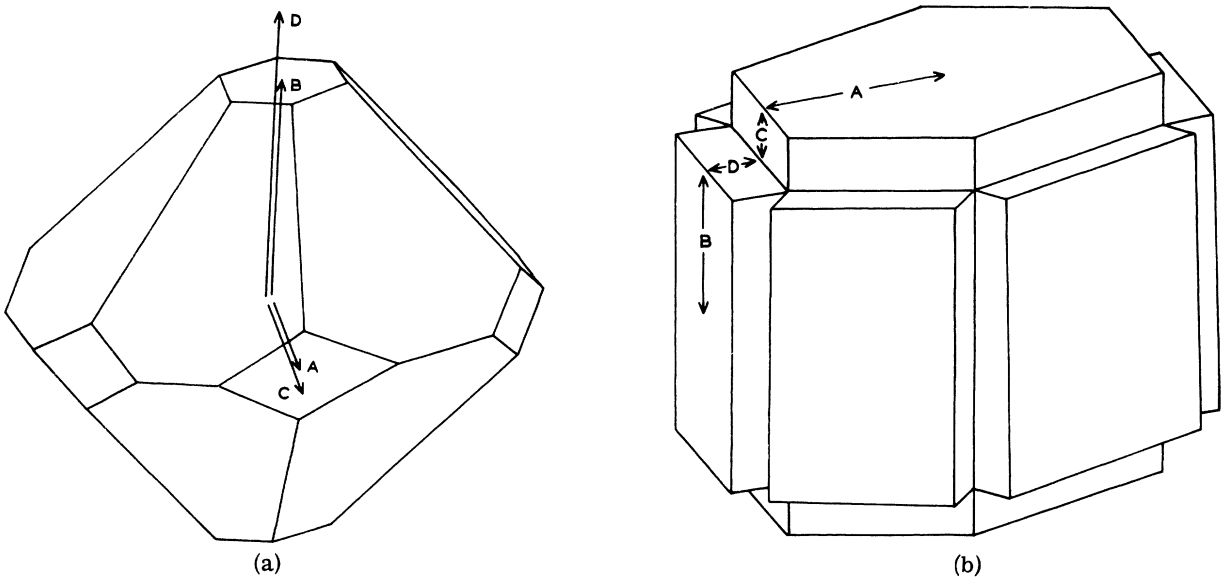

FIG. 3. The plane-faced energy surfaces (PFES) chosen to describe the behavior of hexagonal alloy phases. (a) Surface for $\vartheta < 1.45$; (b) the surface for high ϑ.

tion $i_x \neq i_y$ but one of the components will be the same as those in the first situation.

Application of PFES Method to Hexagonal Alloy Phases

At the lowest electron-to-atom ratio ϑ for which ζ alloys are stable, the phase is comparable to the concentrated fcc primary solid solutions. The $\{0002\}$ faces resemble the $\{111\}$ faces of the fcc structure so one might expect there to be contact between the Fermi surface and the $\{0002\}$ faces of the Jones zone. On geometrical grounds there should also be rather more extensive contact with the $\{10\bar{1}0\}$ faces. One may therefore regard the Fermi surface in extended $\vec{k}$ space as layers of spheres connected by necks in an hexagonal array, each layer being connected by thinner necks to similar layers above and below. At low electron-to-atom ratios (around 1.3) it is reasonable to suppose that there is no overlap into the next zone.

As the band fills, the spheres will expand and the necks grow thicker, becoming a more prominent feature of the arrangement. Eventually overlap will take place into the next zone but for the moment this will be neglected.

It is necessary to choose PFES polygons which can be used to describe this surface. We have been unable to select a single polygon which can be continuously changed over this range and have instead selected two different polygons appropriate to the limiting situations which are shown in Fig. 3. It must be stressed that the selection of the form of the PFES is the only arbitrary choice that is made in this calculation and what is more it turns out that the result is not very sensitive to the exact form chosen, a point made by Allgaier in his original paper.

For the low ϑ model [Fig. 3(a)] with the hexad (c) axis parallel to the z axis (the direction of the magnetic field) the components of the currents i_x and i_y are

$$i_x = \frac{8}{h^3} e^2 E \tau v_x \left[\frac{CD}{2} - (D-B)^2 \frac{C}{D} - (C-A)^2 \frac{D}{C}\right] \times \frac{D}{(C^2+D^2)^{1/2}}, \quad (15)$$

$$i_y = i_x = i_{b,1}, \quad (16)$$

where $\vec{v}$ is the velocity of electrons on the surface. In the present paper it will be assumed that the magnitude of $\vec{v}$ is the same on all faces, which will enable it to be eliminated from the final result. A and B are the distances of the energy zone boundaries from the origin, and C and D are the distance to the apices of the prisms.

The current i_{yx} is conveniently split into two contributions[9]: those from hole-like transitions (the angle between the adjacent faces is greater than π measured on the filled side), and those from electronlike transitions. Figure 4 sketches in an extended-zone scheme the holelike and electronlike transitions.

Then,

$$i^e_{yx} = \frac{8}{h^3}\left[B - (C-A)\right] \times \frac{3\sqrt{3}}{2} \frac{C}{(C^2+D^2)^{3/2}} e^3 E H_z \tau v^2 \quad (17)$$

and

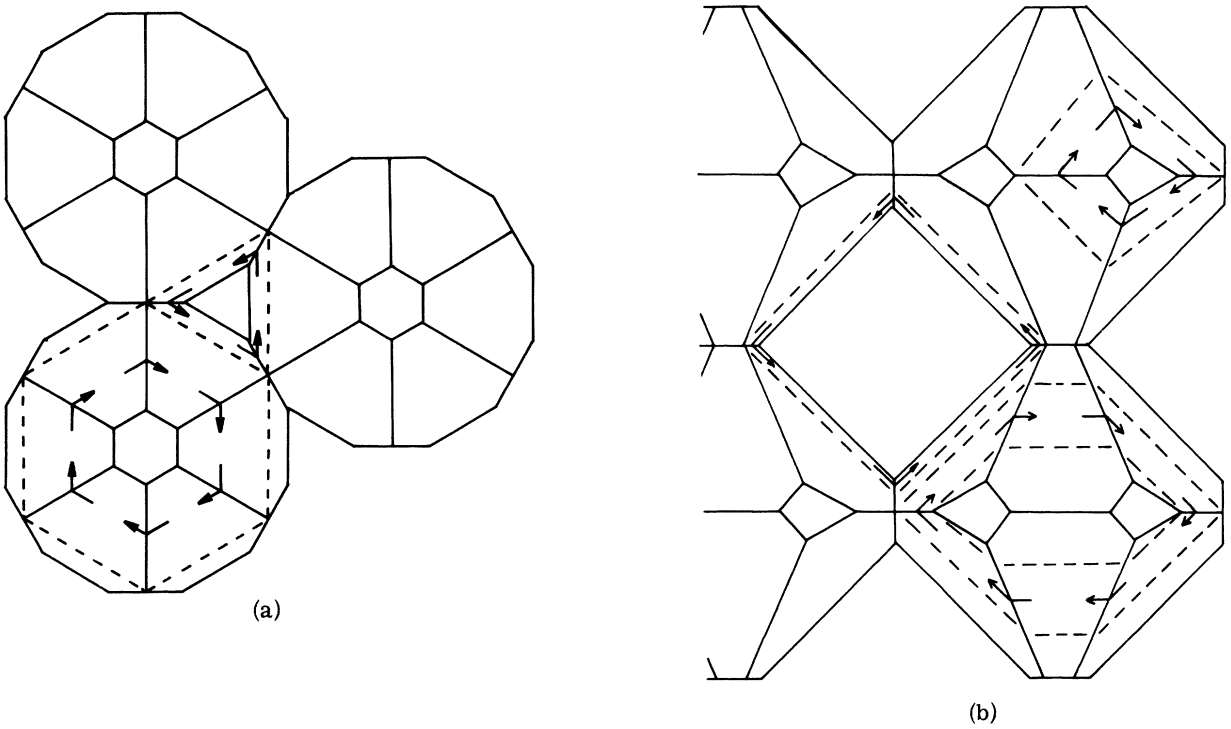

FIG. 4. Electron and hole orbits for the low $\mathfrak{z}$ surface, sketched in the extended zone scheme: (a) $\vec{H}$ parallel to the hexad axis; (b) $\vec{H}$ perpendicular to the hexad axis. Alternative electron paths are shown.

$$i_{yx}^{h}=\frac{8}{h^3}(C-A)\frac{3\sqrt{3}}{2}\frac{C}{C^2+D^2}e^3EH_z\tau v^2 . \tag{18}$$

With the hexad axis normal to the z axis, Eqs. (15)–(18) become

$$i_x=\frac{8}{h^3}e^2\tau E v\left[\frac{CD}{2}-(D-B)^2\left(\frac{C}{D}\right)^2\frac{\sqrt{3}}{4}-(C-A)^2\sqrt{3}\right]\frac{\sqrt{3}C}{(C^2+D^2)^{1/2}} , \tag{19}$$

$$i_y=i_{b,1} , \tag{20}$$

$$i_{yx}^{e}=\frac{8}{h^3}\left[\frac{C}{2}-2(C-A)\right]\frac{\sqrt{3}}{2}\frac{CD}{C^2+D^2}e^3EH_z\tau v^2 , \tag{21}$$

$$i_{yx}^{h}=\frac{8}{h^3}(D-B)\frac{C}{D}\frac{\sqrt{3}}{4}\frac{CD}{C^2+D^2}e^3EH_z\tau v^2 . \tag{22}$$

The volume of the polygon is

$$V=C^2D\sqrt{3}-(D-B)^3\left(\frac{C}{D}\right)^2\sqrt{3}-4\sqrt{3}(C-A)^3\frac{D}{C} \tag{23}$$

and one electron per atom would occupy

$$(3\sqrt{3}/4)A^2B . \tag{24}$$

For the high electron-to-atom ratio model [Fig. 3(b)] the equations corresponding to Eqs. (15) to (18) for the hexad axis parallel to the z axis are

$$i_x=(4/h^3)e^2E\tau v[2\sqrt{3}AD-6BC] , \tag{25}$$

$$i_y=i_x=i_{b,2} , \tag{26}$$

$$i_{yx}^{e}=\frac{4}{h^3}\frac{3\sqrt{3}}{2}De^3EH_z\tau v^2 , \tag{27}$$

$$i_{yx}^{h}=\frac{4}{h^3}\frac{3\sqrt{3}}{2}Be^3EH_z\tau v^2 , \tag{28}$$

and for the case where the hexad axis is normal to the z axis the equations corresponding to Eqs. (19) to (22) are

$$i_x(A>C)=(4/h^3)e^2E\tau v4\sqrt{3}AC , \tag{29}$$

$$i_y=i_{b,2} , \tag{30}$$

$$i_{yx}(C>\tfrac{1}{3}A)=\frac{4}{h^3}\left(\frac{2}{\sqrt{3}}A-2C\right)e^3EH_z\tau v^2 . \tag{31}$$

As the band fills the arms which previously contributed to an open orbit begin to make a holelike contribution

$$i_{yx}(\tfrac{1}{3}A>C)=\frac{4}{h^3}\left[\left(\frac{2}{\sqrt{3}}A-2C\right)+\frac{\sqrt{3}}{2}(A-3C)\right]e^3EH_z\tau v^2 . \tag{32}$$

The volume of this polygon is

$$V = 4\sqrt{3}\,[A^2(B+D)+2ABC]\,. \tag{33}$$

These equations can then be solved numerically with appropriate choice of the dimensions of the surface and the Hall coefficients calculated using Eq. (14). For the first model A was set equal to $1.06B$, and in the second model $(A+C)$ was set equal to $1.06(B+D)$, both these corresponding with ideal axial ratio. In both models C was set equal to D which makes the surface as nearly free electron like as possible. It is then possible to calculate values for $R_{\parallel}$, $R_{\perp}$, and ϑ. These results are shown in Fig. 5.

Experimental Determination of Hall Coefficients

To test the results of the calculation, single crystals of some ζ-phase alloys have been grown using a modified Bridgman technique. The Hall coefficients have been determined using the dc technique described by Lane *et al.*[12] The compositions of the crystals and the experimental values of the Hall coefficient are listed under "Single Crystals" in Table I.

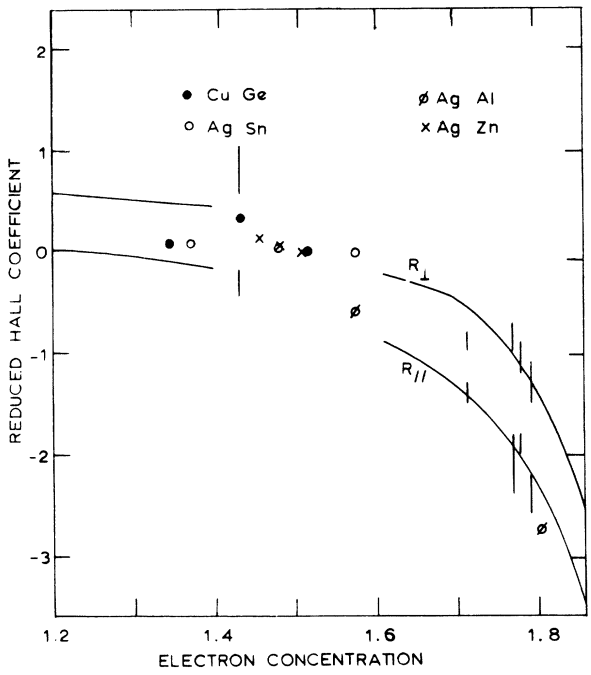

FIG. 5. Calculated and measured Hall effects for ζ-phase alloys. The full curves are calculated from the surfaces shown in Fig. 3: the left-hand pair are for the surface shown in Fig. 3(a) and the right-hand pair for the surface shown in Fig. 3(b). The experimental results are those listed in Table I. The coefficients for the single-crystal specimens are shown as vertical lines where length indicates the experimental uncertainty; the low ϑ values are for Cu-Ge single crystals (Ref. 6) and the high ϑ values for Ag-Al single crystals. The points are for polycrystalline specimens of undetermined texture and should therefore lie somewhere between the curves representing the separate coefficients.

TABLE I. Measured Hall coefficients. All the polycrystalline specimens were cast and annealed but ground rather than rolled so as to preserve the as-cast texture. The copper germanium alloy marked with an asterisk was the result of a failed single-crystal run and was therefore large grain sized. There was a possibility of oxidation of the zinc-based alloys due to the method of preparation. For this reason the specimen marked with two asterisks was oxidized for 6 h at 400 °C to determine the importance of this. The alloys labeled (a) are ϵ phase: the remainder are ζ phase. R_{FE} is the value of the Hall coefficient calculated from the free-electron theory.

Single Crystals			
Alloy system	ϑ	$R_{\parallel}/R_{FE}$	$R_{\perp}/R_{FE}$
Silver-aluminum	1.712	-1.4 ± 0.1	-0.9 ± 0.1
	1.768	-2.1 ± 0.3	-0.8 ± 0.2
	1.776	-1.9 ± 0.1	-1.05 ± 0.15
	1.791	-2.4 ± 0.2	-1.3 ± 0.2
Copper-germanium (Ref. 6)	1.42	-0.25 ± 0.1	0.8 ± 0.25
Polycrystals			
Alloy system	ϑ	R/R_{FE}	
Silver-aluminum	1.57	-0.53	
	1.80	-2.86	
Copper-germanium	1.36	0.063	
	1.42	0.3*	
	1.50	0.024	
Silver-tin	1.39	0.088	
	1.48	0.055	
	1.57	0.034	
Silver-zinc	1.463	0.23 ± 0.03	
(Ref. 13)	1.486	0.18 ± 0.02	
	1.507	0.18 ± 0.02	
(a)	1.83	0.10	
Zinc-copper (a)	1.828	0.085	
(a)	1.855	0.12	
(a)	1.850	0.2**	
(a)	1.867	0.155	

It is not easy to grow crystals of these alloys, since most form by a peritectic reaction; and in the case of ϵ-phase alloys it has so far been impossible to grow single crystals. However, as Lane has shown, it is reasonable to expect that for polycrystalline specimens of hexagonal metals a Hall coefficient will be obtained which will have a value somewhere between those of the two single-crystal coefficients, the exact value depending on the orientation distribution in the polycrystal. Thus, results derived from polycrystals can be used to give a semiquantitative indication of the correspondence between experiment and theory. Data from polycrystalline specimens[13] are listed under "Polycrystals" in Table I.

These results, and the single-crystal coefficients of Hitchcock and Stringer,[6] are included in

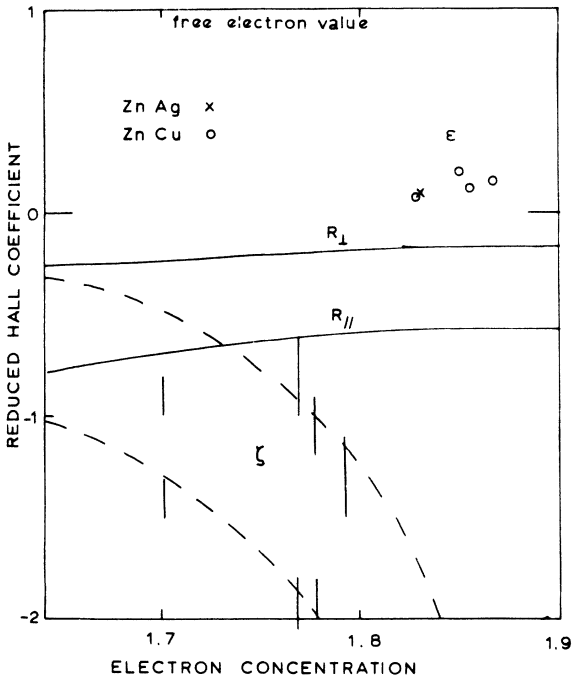

FIG. 6. Calculated and measured Hall effects for ϵ-phase alloys. The dashed curves are those calculated without overlap for the surface shown in Fig. 3(b); the ζ-phase single crystal results for Ag-Al crystals are included as vertical lines. The full curves are calculated assuming the onset of overlap. The experimental points are for polycrystalline specimens of undertermined texture, and should then lie somewhere between the curves representing the separate coefficients. It is clear that there is considerable overlap, and that the simple calculation may have underestimated the amount.

Figs. 5 and 6. It is apparent that there is very satisfactory agreement in the case of the ζ-phase systems shown in Fig. 5; the ϵ-phase results shown in Fig. 6 are discussed later.

Discussion

At first the choice of a PFES seems unrealistic because of the sharp changes in direction at the edges. However, this is equivalent to the summation of the infinitesimal changes in direction associated with movement on a real, smoothly curved, Fermi surface and for the low-field Hall coefficient there will thus be little difference: the PFES simply replaces a difficult integral with a relatively simple, small number of summations, the only error being that the edges do not satisfy the low-field condition. To obtain an accurate result it is only necessary that the PFES should reasonably closely follow the actual Fermi surface. For example, Allgaier[9] demonstrated that a regular polygon having 24 faces gave a value for the Hall coefficient within 10% of the value calculated for a spherical Fermi surface by conventional methods.

The results of the present analysis show a most encouraging agreement with the experiment, and it should be noted that although the two forms of PFES used are quite different they may be joined to form a reasonably smooth continuous curve. This reinforces the point that the detailed form of the PFES is not critical. Furthermore, the calculation involves no other arbitrarily assignable parameters.

It seems very likely that overlap into the second energy band will occur within this range of ϑ and the new states will produce their own contributions to the Hall coefficients. The magnitude of the effects can be estimated as follows. When overlap first occurs a small fraction of newly filled states must be in the second band. By the time the electron-to-atom ratio has risen to its value for a full band (taken here to be 2, the semiquantitative result we obtain is insensitive to the actual value), half the newly filled states will be in the second band. Thus, the upper limit to the effect of filling new states is obtained by allowing half the electrons to occupy states in the second band after the onset of overlap.

If the new states are said to be square blocks of dimension $2F \times 2F \times F$ on each zone boundary face, then the volume of the new states would be

$$V' = 32F^3 . \tag{34}$$

The contributions of these states to the currents would be

$$i'_x = i'_y = 64F^2e^2E\tau v/h^3 , \tag{35}$$

$$i'_{xy} = 8Fe^3EH_z\tau v^2/h^3 . \tag{36}$$

These must be added to the earlier contributions, picking values of F which make

$$V' = V - V_0 ,$$

where V is the volume of states filled in the first zone, and V_0 is the volume of states filled at the onset of overlap.

Massalski and King[14] have suggested that overlap across the $\{10\bar{1}0\}$ faces occurs at an electron-to-atom ratio of approximately 1.5 in silver-based alloys, from their lattice-parameter data. An estimate of the possible change in Hall coefficient is shown in Fig. 6. In this case, as the model is becoming unrealistic for electron-to-atom ratios of less than about 1.6, overlap was considered to start at an electron-to-atom ratio of 1.66 (roughly corresponding to the composition at which Massalski and King's lattice-parameter data for silver-aluminium shows the discontinuity attributed to the onset of overlap). However, the general features of the effect will be the same whenever the onset of overlap. The effect of there being only

a small proportion of states filled in the new zone initially will lessen the initial change. Since the simple model seems to fit the experimental results for the ζ-phase alloys better than this it seems that the initial degree of overlap is very small. However, the results for the ϵ-phase polycrystals shown in Fig. 6 are clearly inconsistent with the model without overlap, and indeed suggest that the simple modification above underestimates the contribution of the overlap.

There has been no attempt to include axial ratio variations explicitly in these calculations. To do so would be simple, but since there is a degree of arbitrariness in the relative contact areas with the $\{0002\}$ and $\{10\bar{1}0\}$ faces of the zone boundary, the relatively small effect of a change of axial ratio would be concealed. This effect must be quantified before the technique is applied to systems where there is a wide variation of axial ratio.

The assumptions that both the relaxation time and the velocity are isotropic are clearly questionable, although the satisfactory agreement with experiments suggests that in this case they are correct. However, in other cases (for example, the pure group-II metals and dilute alloys based on them), these assumptions are unlikely to be correct, and in that event the calculations will involve some more arbitrary aspects. On balance, however, the PFES method would appear to be an extremely useful method for these alloy systems, and suggests that study of the Hall effect may give useful information on Fermi-surface effects in hexagonal alloys. In particular, the results obtained suggest that there is very little overlap in ζ-phase alloys, but quite extensive overlap in the ϵ phase.

ACKNOWLEDGMENTS

One of the authors (P. H. C.) wishes to acknowledge the receipt of an S. R. C. studentship. We are grateful to Dr. Allgaier for his comments and helpful suggestions.

[1]J. K. Logan and J. A. Marcus, Phys. Rev. **88**, 1234 (1952).
[2]H. B. G. Casimir, Rev. Mod. Phys. **17**, 343 (1945).
[3]M. Kohler, Ann. Phys. (N.Y.) **20**, 878 (1934).
[4]R. G. Chambers, in *The Physics of Metals*, edited by J. N. Ziman (Cambridge U. P., Cambridge, England, 1969), Vol. 1, p. 175.
[5]J. S. Dugdale and L. D. Firth, J. Phys. C **2**, 1272 (1969).
[6]A. H. Hitchock and J. Stringer, Phys. Status Solidi **3**, 755 (1970).
[7]M. Tsuji and M. Kunimune, J. Phys. Soc. Jap. **18**, 1569 (1963).
[8]R. S. Allgaier, Phys. Rev. **158**, 699 (1967).
[9]R. S. Allgaier, Phys. Rev. **165**, 775 (1968).
[10]R. S. Allgaier, Phys. Rev. B **2**, 3869 (1970).
[11]C. Goldberg, E. Adams, and R. Davis, Phys. Rev. **105**, 865 (1957).
[12]G. S. Lane, A. S. Huglin, and J. Stringer, Phys. Rev. **135**, A1060 (1964).
[13]S. Noguchi, J. Phys. Soc. Jap. **17**, 1844 (1962).
[14]T. B. Massalski and H. W. King, Prog. Mater. Sci. **10**, 3 (1963).